JTTEE5 18:619–632
DOI: 10.1007/s11666-009-9371-9
1059-9630/$19.00 © ASM International

High-Temperature Corrosion Studies of HVOF-Sprayed Cr_3C_2-NiCr Coating on SAE-347H Boiler Steel

Manpreet Kaur, Harpreet Singh, and Satya Prakash

(Submitted January 28, 2009; in revised form July 3, 2009)

Cr_3C_2-NiCr coating was deposited on SAE-347H boiler steel by high velocity oxy fuel (HVOF) spray process. Subsequently, high-temperature corrosion behavior of the bare and coated boiler steel was investigated at 700 °C for 50 cycles in Na_2SO_4-82$Fe_2(SO_4)_3$ molten salt, as well as air environments. Weight-change measurements after each cycle were made to establish the kinetics of corrosion. X-ray diffraction, field emission-scanning electron microscopy/energy dispersive spectroscopy, and x-ray mapping analyses were performed on the exposed samples to analyze the oxidation products. The bare 347H steel suffered accelerated oxidation during exposure at 700 °C in the air as well as the molten salt environment in comparison with its respective coated counterparts. The HVOF-spray Cr_3C_2-NiCr coating was found to be successful in maintaining its adherence in both the environments. The surface oxide scales were also found to be intact. The formation of chromium rich oxide scale might have contributed for the better hot corrosion/oxidation resistance in the coated steel.

Keywords coatings, Cr_3C_2-NiCr, hot corrosion, HVOF-spray, oxidation

1. Introduction

Among the thermal spraying technologies used to deposit cermet coatings, high velocity oxy fuel (HVOF) has been proved to be particularly effective, producing very dense coatings with adhesion to the substrate and high hardness. The process is a low-temperature method compared with other techniques, it requires minimal base metal preparation and it can be directly applied to the working tools. In the HVOF thermal spray technology, oxygen and liquid fuel are combusted under high pressure in a chamber and the combustion products are accelerated through a converging-diverging nozzle (Ref 1). The powder, fed into the hot stream of gases, is heated and then is accelerated on the substrate at very high speed (650-850 m/s) (Ref 2). Because of the high velocity associated with a relatively low flame temperature, HVOF is considered a valid process to deposit cermet coatings of low porosity content (about 1%): in particular, HVOF allows creating denser and less oxidized coatings than conventional thermal spray technologies (Ref 3), and no significant thermal and mechanical alterations of the substrate are usually observed. The most common HVOF cermet coatings are WC-Co, WC-CoCr, and Cr_3C_2-NiCr systems. Cr_3C_2-NiCr coatings show comparatively poorer tribological properties, but they are much more resistant at high temperatures and in aggressive environments: for these reasons they are used, for example, in steam turbine blades or in boiler tubes for power generation (Ref 4).

Thermally sprayed Cr_3C_2-NiCr coatings are used in applications that demand protection against surface degradation due to oxidation, wear, and corrosion under severe conditions of excessive heat and load (Ref 5). These coatings show good tribological properties in rigorous working conditions such as at high temperatures or in aggressive environments, for example in steam turbine blades or in boiler tubes for power generation. These coatings maintain their high wear and corrosion resistance up to 1253 K and can be used to improve the performance life of components working at elevated temperatures (Ref 6, 7). Different studies indicate that Cr_2O_3 (protective oxide) is preferentially formed at high temperatures on the coating surface and so prevents oxidation of the whole coating. Thermogravimetric studies indicate that at 873 K the oxidation of Cr_3C_2-NiCr starts and at temperatures as high as 1073 K is still low (Ref 8). As a carbide form, the Cr_3C_2-NiCr coatings sprayed by HVOF process can be recommended as a promising coating for the heat exchanger pipes (Ref 9).

The objective of this work is to study the high-temperature corrosion and oxidation behavior of SAE-347H boiler material with and without HVOF-sprayed Cr_3C_2-NiCr coatings under cyclic conditions at the temperature of 700 °C. Knowledge of the reaction kinetics and the nature of the surface scales formed during the high-temperature corrosion (hot corrosion) and oxidation are important for evaluating the materials for their use and

Manpreet Kaur, Baba Banda Singh Bahadur Engineering College, Fatehgarh Sahib, India; **Harpreet Singh**, Mechanical Engineering Department, Indian Institute of Technology, Ropar, Roopnagar 140001, Punjab, India; and **Satya Prakash**, Indian Institute of Technology Roorkee, Roorkee, India. Contact e-mail: hn1998@gmail.com.

degradation characteristics in high-temperature applications (Ref 10). The high-temperature corrosion tests have been conducted in the molten salt environment comprising of Na_2SO_4-82$Fe_2(SO_4)_3$ salts. This environment is usually found in coal-fired boilers (Ref 9). The high-temperature oxidation testing in air is also necessary to get information regarding the adhesion of the coating to the substrate under thermal cyclic loading.

2. Experimental

2.1 Deposition of Coating

The SAE-347H boiler material was procured from Guru Gobind Singh Super Thermal Power Plant, Ropar, Punjab (India). The actual chemical composition of the substrate steel was determined by spectroscopy. The actual (as measured) and nominal compositions of the steel are given in Table 1. Specimens with dimensions of approximately 20 mm × 15 mm × 5 mm were cut from this material. The specimen were polished with SiC papers down to 180 grit and subsequently grit blasted by alumina (grit 60) before the application of the coatings by HVOF process. Commercially available Cr_3C_2-NiCr coating powder was deposited on this boiler steel by the HVOF process. The coating powder has a particle size in the range of $-45 + 15$ μm.

The SEM morphology of the powder has been reported in Fig. 1. The coating powder is found to be in the form of lumps of irregular sized particles. Most of the particles have a spherical morphology. The Cr_3C_2-NiCr coatings were then deposited on the boiler steel specimens at Metallizing Equipment Company Pvt Ltd. Jodhpur (India) with their commercial HVOF (HIPOJET-2100) apparatus operating with oxygen and liquid petroleum gas (LPG) as input gases. The coatings were deposited on all the sides of the specimens. The spraying parameters adopted by the manufacturer are given in Table 2. The substrate steels were cooled by compressed air jets during and after spraying. Coating thickness was kept in a range of 225 ± 25 μm.

2.2 Characterization of the Coating

The coated samples were cloth wheel polished and then subjected to the XRD analysis by using a Bruker AXS D-8 Advance Diffractometer (Germany) with Cu$K\alpha$ radiation and nickel filter at 20 mA under a voltage of 35 kV. The SEM/EDS analysis of the samples was carried out by field emission-scanning electron microscope (FE-SEM, FEI, Quanta 200F Company) attached with EDS Genesis software (Made in Czech Republic) to characterize the surface morphology and composition of the coating. The SEM micrographs along with EDS spectrum were taken with an electron beam energy of 20 keV.

2.3 Oxidation and Molten Salt Corrosion Tests

Cyclic oxidation studies were performed on the samples in air as well as in the simulated environment of boilers [Na_2SO_4-82$Fe_2(SO_4)_3$], with each cycle consisting of 1 h of heating at 700 °C in a silicon carbide tube furnace followed by 20 min of cooling at the room temperature for 50 cycles. The aim of cyclic loading is to create conditions for the accelerated corrosion testing. Moreover, the cyclic conditions resemble the actual industrial conditions where the plants are operated and shut down frequently for many reasons. These studies were performed for the bare and coated samples to obtain a comparative database. All the specimens were polished down to 1-μm alumina cloth wheel polishing before the oxidation/corrosion studies. In the case of molten salt corrosion testing, a salt coating of uniform thickness weighing 3-5 mg/cm^2 of Na_2SO_4-82$Fe_2(SO_4)_3$ paste was applied with a camel hairbrush on

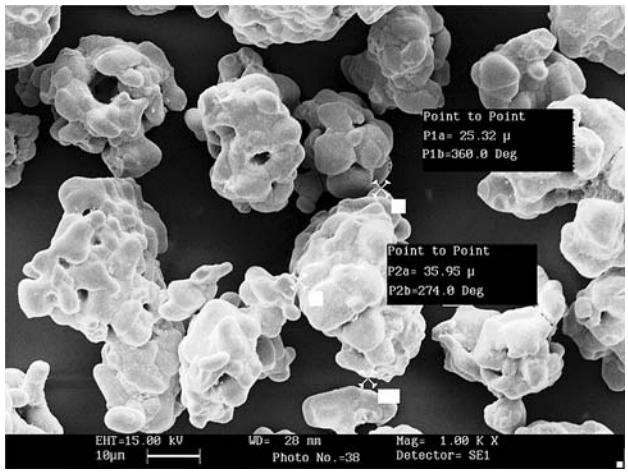

Fig. 1 Morphology of the Cr_3C_2-NiCr powder

Table 2 Spray parameters as employed during the HVOF spraying

Oxygen flow rate, SLPM	250
Fuel (LPG) flow rate, SLPM	60-70
Air flow rate, SLPM	600
Spray distance, inches	6-7
Powder feed rate, g/min	25

SLPM standard litres per minute

Table 1 Chemical composition (wt.%) of the steel

Type of Steel	ASTM code	Composition	C	Mn	Si	S	P	Cr	Ni	V	Cu	Ti	Sn	Fe
347H	SAE-347H	Nominal	0.04-0.1	2.0	0.75	0.03 max	0.04 max	17-20	9-13	...	...	...	...	Bal.
		Actual	0.0558	1.792	0.6392	0.00715	0.01935	17.72	9.910	0.0457	0.0554	0.0125	0.0056	Bal.

the preheated samples (250 °C). Weight-change measurements were taken at the end of each cycle using an electronic balance with a sensitivity of 1 mg. Any spalled scale was also included at the time of weighing to determine the total rate of corrosion. Efforts were made to formulate the kinetics of the oxidation/corrosion. The exposed samples were analyzed using FE-SEM/EDS and XRD for surface analysis of their scales. To identify the cross-sectional details, the samples were sectioned, mounted in transoptic powder and subjected to mirror polishing using emery papers of 220, 400, 600 grit sizes and subsequently on 1/0, 2/0, 3/0, and 4/0 grades, successively. Fine polishing was done to obtain a mirror finish using diamond paste. The polished samples were characterized to obtain their cross-sectional morphology and compositions by using FE-SEM/EDS. The EDS Genesis software was used to calculate the composition of the elements in the coatings from their corresponding emitted x-ray peaks. Cross-sectional x-ray maps of the various elements present in the specimens were also taken on the same machine.

3. Results

3.1 SEM/EDS Analysis of As-Sprayed 347H Boiler Steel

The surface scale morphology of HVOF-spray Cr_3C_2-NiCr coated 347 H boiler steel has been shown in Fig. 2. The as-sprayed coating is found to have a morphology consisting of irregular shaped splats. The splats have variable shapes and sizes, which are interconnected. Some superficial voids can also be seen in the microstructure. The EDS analysis of the coating surface indicates the presence of mainly Cr and Ni elements in the coating compositions. There is a presence of small amount of O also, which indicates that some oxides may have also been formed in the structure.

3.2 XRD of As-Sprayed 347H Boiler Steel

The XRD analysis of the HVOF-spray Cr_3C_2-NiCr coated 347H boiler steel has been compiled in Fig. 3. The XRD peaks of as-sprayed 347H boiler steel reveal the presence of Cr_3C_2, Cr_7C_3, and Cr_3Ni_2 as main phases. Some medium intensity peaks indicating the presence of CrNi phase are also revealed by the XRD analysis.

3.3 Visual Observations and Weight-Change Analysis

Micrographs of the bare and HVOF-spray Cr_3C_2-NiCr coated 347H steel after exposure to cyclic oxidation in air at 700 °C for 50 cycles have been shown in Fig. 4. The oxide scale formed on the bare 347H boiler steel (Fig. 4a) was observed to be brown in color. Initially, after the very first cycle, some light blue spots were observed on the surfaces of the specimen. Small black spots on the sides were also found after the eighth cycle. With the passage of the exposure time, the color of the scale changed to golden brown with black spots. The color turned to brown and the black spots vanished toward the end of cycles. Whereas, the HVOF-spray Cr_3C_2-NiCr coated 347H boiler steel was initially gray in color. The color changed to dark gray after the first cycle with indications of few white spots which vanished afterward toward the end of the exposure. The scale continued to become darker toward blackish gray appearance with the increase in the exposure. The scale showed a tendency to spall from some of the corners of the sample as could be seen in Fig. 4(b). However, the coating, in general, showed good adherence to the boiler steel with no tendency for spallation of oxide scale from major surface area.

The photographs of the bare and HVOF-spray Cr_3C_2-NiCr coated 347H steel after exposure to the molten salt corrosion at 700 °C for 50 cycles have been shown in Fig. 5. In the hot-corroded bare 347H boiler steel, a gray colored scale appeared on the surface from the first cycle. With the increase in the exposure time, some brown patches appeared on the shiny lustrous gray scale by the end of the study. Only marginal spallation of the scale in the powder form was observed as could be seen in the boat. The exposed specimen has been depicted in Fig. 5(a). The HVOF-sprayed Cr_3C_2-NiCr coated 347H boiler steel, when subjected to the salt environment indicated the formation of a gray colored scale after the end of very first

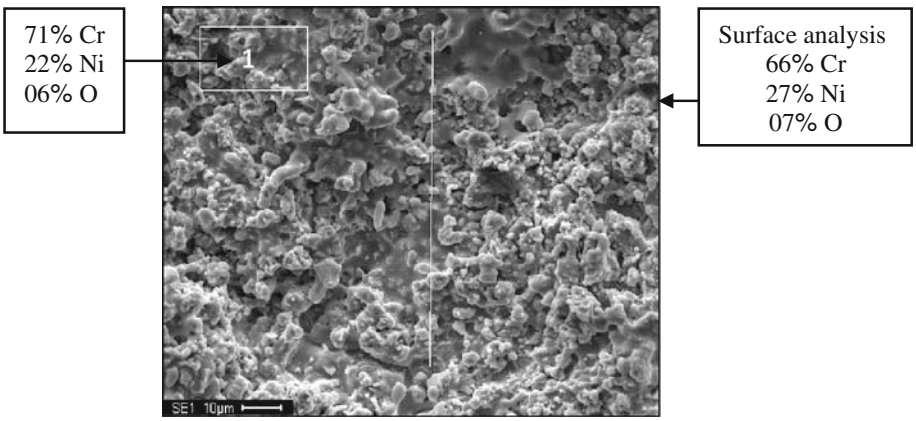

Fig. 2 Surface scale morphology and EDS analysis for the HVOF spray Cr_3C_2-NiCr coated 347H boiler steel in as-sprayed condition

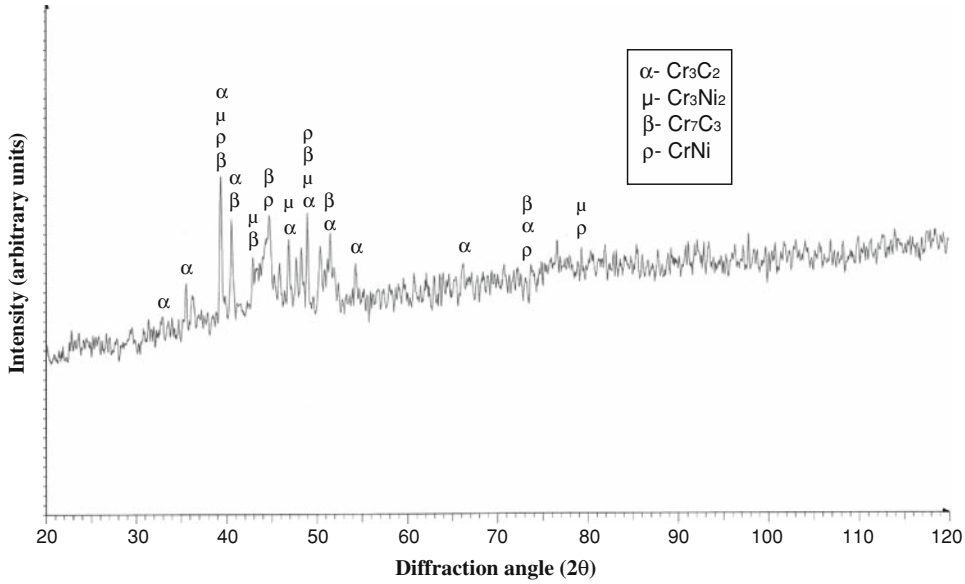

Fig. 3 X-ray diffraction pattern for the HVOF spray Cr_3C_2-NiCr coated 347H boiler steel

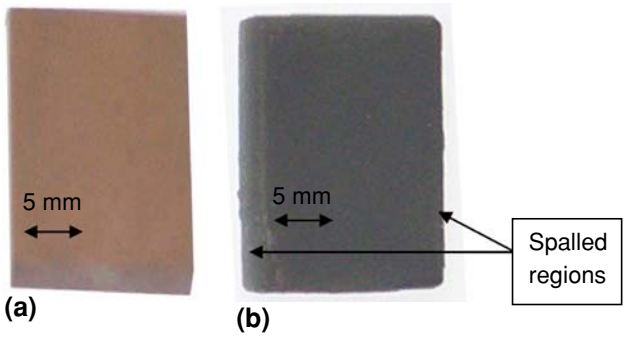

Fig. 4 Macrographs of (a) uncoated and (b) HVOF spray Cr_3C_2-NiCr coated 347H boiler steel subjected to cyclic oxidation in air at 700 °C for 50 cycles

cycle, with salt crystals scattered on the sides. After the 30th cycle, the oxide layer showed a little tendency to spall from some of the sides. However, the coating was intact over most of the surface area of the specimen.

The weight-change/unit area data for all the investigated cases have been plotted against the number of cycles in Fig. 6. It is evident that the coated as well as the bare steel has shown overall weight losses in both the given environments. It can be inferred from the plots that the uncoated 347H boiler steel showed lesser air oxidation resistance in comparison to its coated counterpart. It has been seen that the overall weight loss for the steel got reduced by 15% after the deposition of the coating (Fig. 7).

Similarly the uncoated 347H boiler steel when subjected to the hot corrosion experimentation in Na_2SO_4-$Fe_2(SO_4)_3$ salt at 700 °C for 50 cycles showed loss of weight, during the entire period of study. The rate of oxidation went on increasing with the progress of the

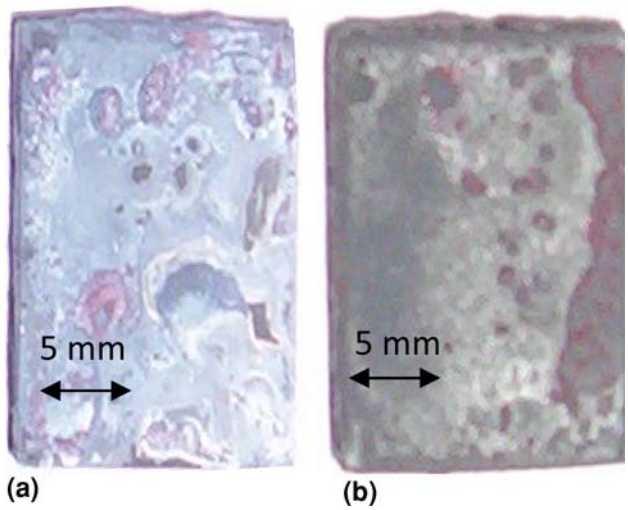

Fig. 5 Macrographs of (a) uncoated and (b) HVOF spray Cr_3C_2-NiCr coated 347H boiler steel subjected to cyclic oxidation in Na_2SO_4-82%$Fe_2(SO_4)_3$ at 700 °C for 50 cycles

oxidation study. Whereas, in the HVOF-sprayed Cr_3C_2-NiCr coating, rapid oxidation rate was not observed and it showed comparatively lesser weight loss with the progress of exposure time. The overall weight loss for the steel got reduced by 53% after the deposition of the coating (Fig. 7).

3.4 XRD Analysis

The various phases identified from the x-ray diffraction (XRD) patterns of the oxidized bare 347H steel in air at 700 °C for 50 cycles are shown in Fig. 8. FeNi and Ni, Fe were observed as the main phases, whereas Fe_2O_3 and Cr_2O_3 were also revealed in the oxide scale. Further, the

diffractograms (Fig. 9) of the surface oxides formed on the Cr_3C_2-NiCr coated 347H steel indicated the formation of Cr_2O_3 and Cr_7C_3 as very strong phases, Cr_3C_2 as a strong phase and Cr_2C, Cr_3O_4, and Cr_3Ni_2 as medium/low intensity phases.

The XRD diffractograms for the uncoated and coated boiler steel after exposure to salt at 700 °C for 50 cycles are depicted in Fig. 10 and 11, respectively, on reduced scales. In the hot-corroded bare 347H steel, Fe_2O_3 and Cr_2O_3 were found to be the strong phases. Also, NiO and Na_2O were observed as weak phases. Whereas, for the Cr_3C_2-NiCr coated boiler steel, the XRD analysis has indicated the formation of Fe_2O_3 and Cr_2O_3 as very strong phases, Cr_7C_3 as a strong phase, and Cr_2C as a medium phase in the oxide scale.

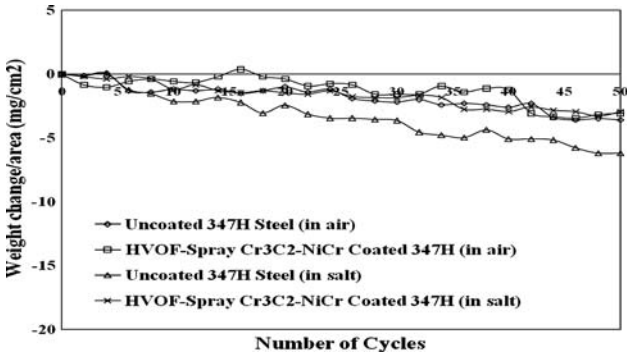

Fig. 6 Weight change vs. number of cycles plots for the uncoated and HVOF spray Cr_3C_2-NiCr coated 347H boiler steel subjected to cyclic oxidation for 50 cycles in air and in Na_2SO_4-Fe_2 $(SO_4)_3$ salt environments at 700 °C

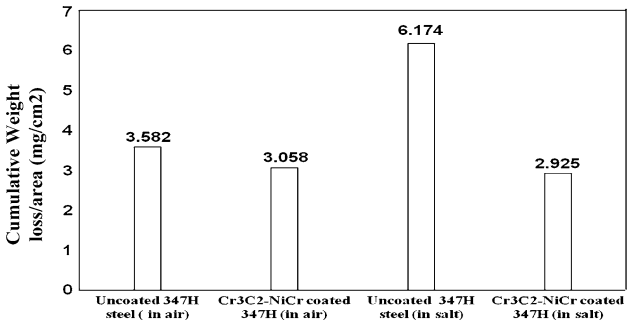

Fig. 7 Bar chart showing cumulative weight loss per unit area for the uncoated and HVOF spray Cr_3C_2-NiCr coated 347H boiler steel subjected to cyclic oxidation for 50 cycles in air and in Na_2SO_4-Fe_2 $(SO_4)_3$ salt environments at 700 °C

3.5 FE-SEM/EDS Analysis

3.5.1 Air Oxidation. FE-SEM micrographs with EDS analysis for the Cr_3C_2-NiCr coated and bare boiler steel after cyclic oxidation in air for 50 cycles at 700 °C are shown in Fig. 12. The surface scale developed on the oxidized boiler steel consists of a globular phase, showing tendency to align along a particular direction in the form of streaks. The density of the globules is different along different streaks. The EDS analysis indicates that the scale is mainly consisting of Fe, Cr, and O, showing the possibility of formation of oxides of Fe and Cr in the scale. Presence of small amounts of Mn and Ni is also revealed. Whereas, the morphology of oxidized Cr_3C_2-NiCr coated boiler steel appears to be consisting of spongy nodules (Fig 12b). The EDS analysis of the scale revealed the possible formation of Cr_2O_3 and NiO as the principal phases.

3.6 Molten Salt Oxidation

The SEM micrograph (Fig. 13a) for the hot-corroded 347H steel reveals an oxide scale consisting of globules, having, by and large, uniform size distribution. The overall EDS surface analysis reveals that the oxide scale consists mainly of Fe, O, and Cr. The matrix of the scale at point 2

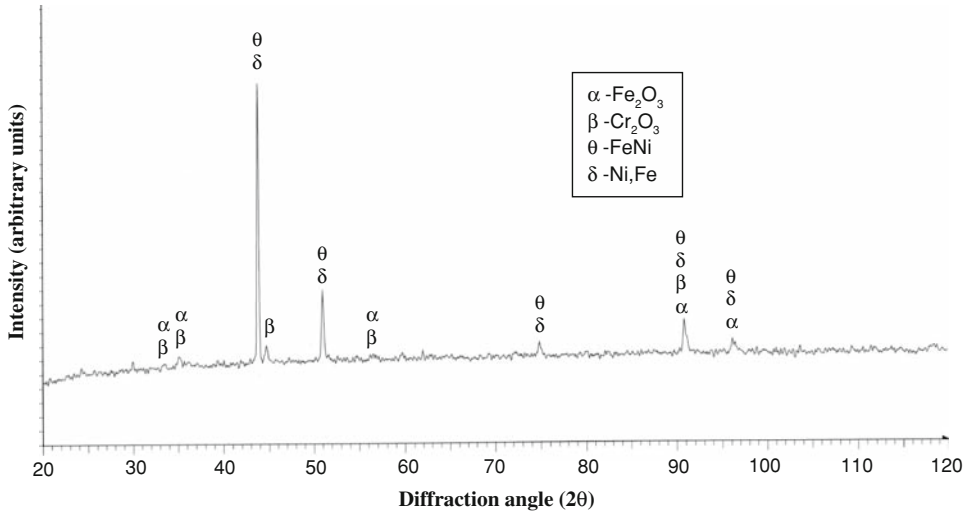

Fig. 8 X-ray diffraction pattern for the uncoated 347H boiler steel subjected to cyclic oxidation in air at 700 °C for 50 cycles

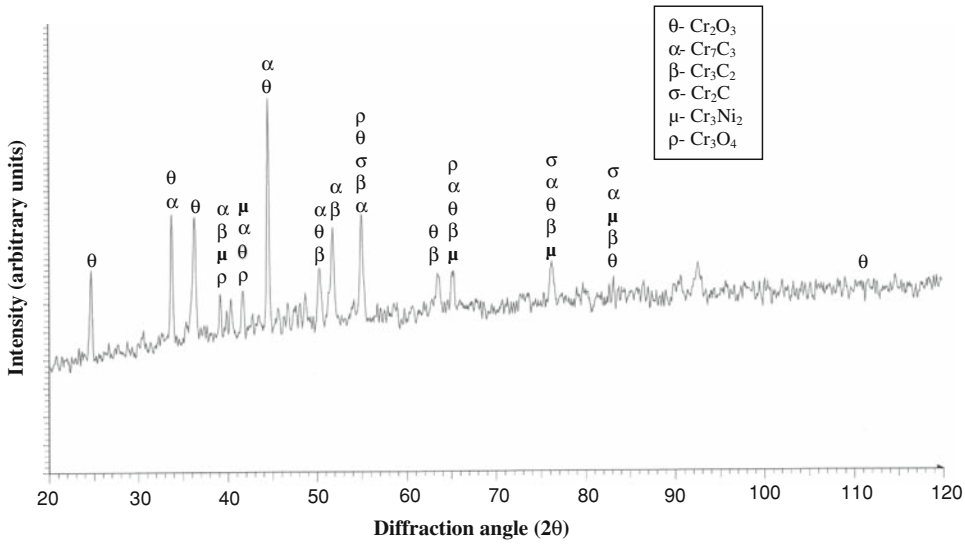

Fig. 9 X-ray diffraction pattern for the HVOF spray Cr_3C_2-NiCr 347H boiler steel subjected to cyclic oxidation in air at 700 °C for 50 cycles

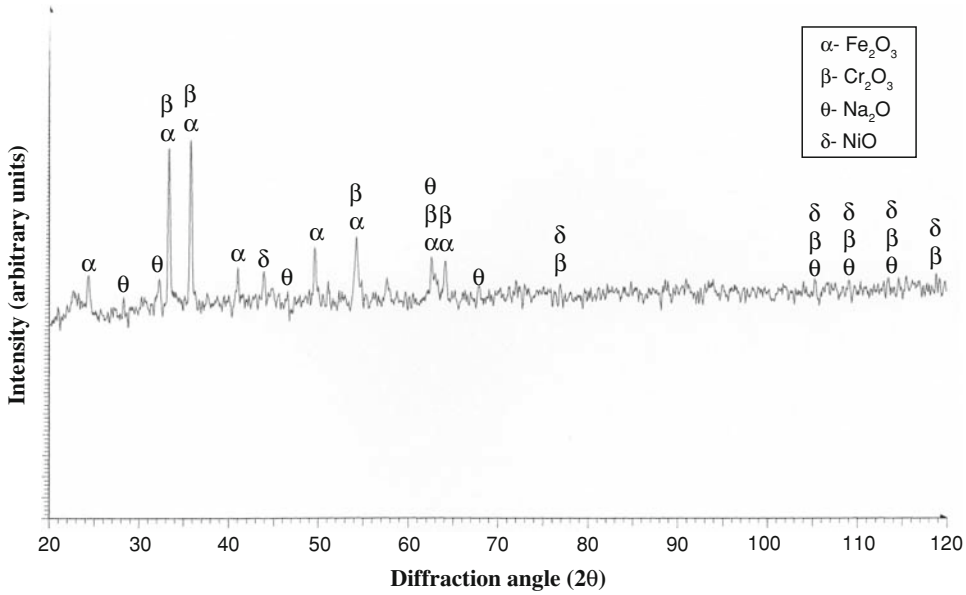

Fig. 10 X-ray diffraction pattern for the uncoated 347H boiler steel subjected to cyclic oxidation in Na_2SO_4-82%Fe_2 $(SO_4)_3$ salt at 700 °C for 50 cycles

is consisting mainly of Fe, O, and Cr along with Na. The scale is having a significant amount of Na (22%) at point 1, along with O, Fe, and Cr as other dominant constituents. On the other hand, the hot-corroded Cr_3C_2-NiCr coated 347H steel has an irregular scale with an amorphous appearance. The EDS compositions of the scale at the points of measurements show wide variations (Fig. 13b) in the composition of the scale. The presence of Na, S, and O at the point 3 indicates the existence of unreacted salt (Na_2SO_4) in the scale. The EDS analysis of bulk oxide scale indicates that the oxide scale mainly contains Fe, O, Na, and Cr.

3.7 Cross-Sectional Analysis of the Scales

3.7.1 Air Oxidation. Oxide scale morphologies along with variation of elemental composition across the cross section of the HVOF spray Cr_3C_2-NiCr coated and uncoated 347H steel subjected to cyclic oxidation in air at 700 °C after 50 cycles have been shown in Fig. 14. The scale formed on the surface of uncoated steel has a dense appearance with a nearly uniform thickness as shown in Fig 14(a). The scale mainly consists of iron along with significant amounts of chromium, nickel, and carbon. Presence of oxygen has also been indicated throughout the

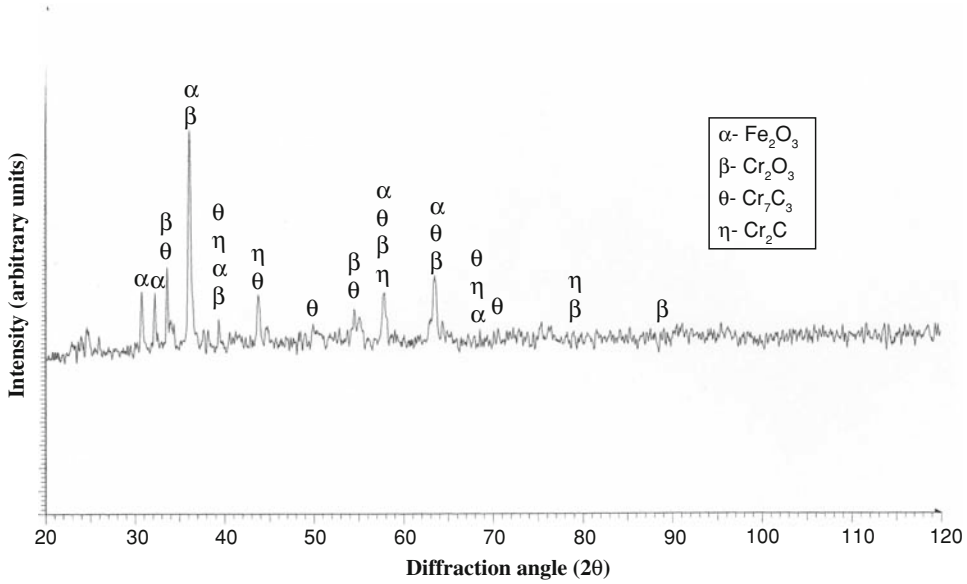

Fig. 11 X-ray diffraction pattern for the HVOF spray Cr_3C_2-NiCr 347H boiler steel subjected to cyclic oxidation in Na_2SO_4-82%$Fe_2(SO_4)_3$ salt at 700 °C for 50 cycles

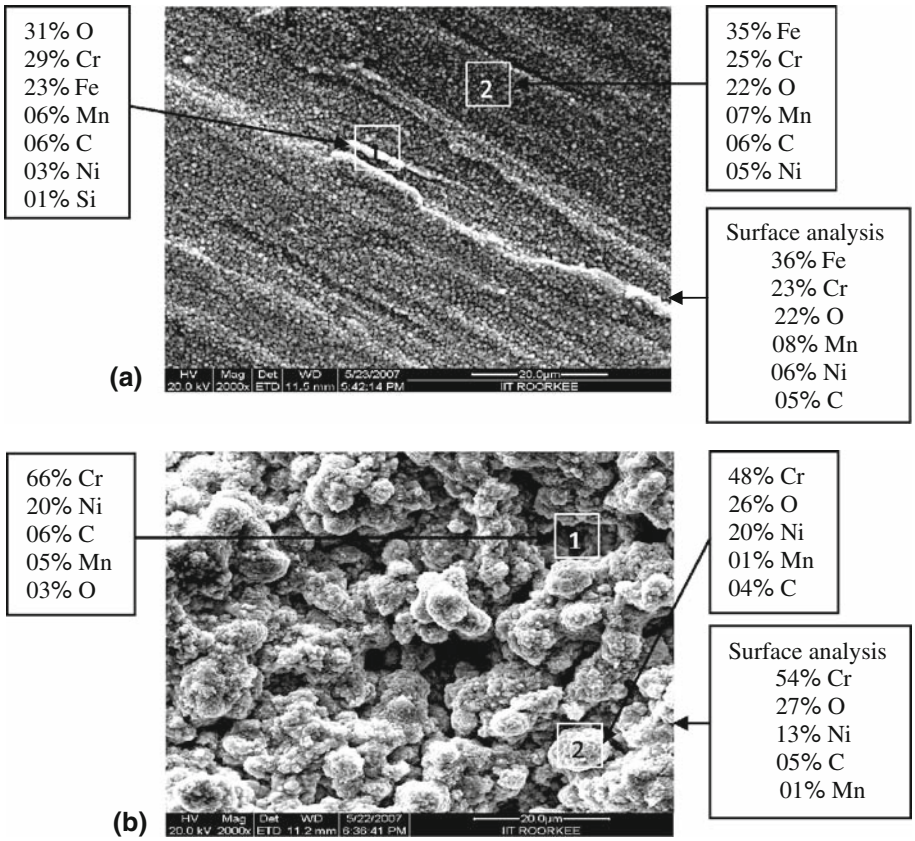

Fig. 12 Surface scale morphology and EDS analysis for the 347H boiler steel subjected to the cyclic oxidation in air at 700 °C for 50 cycles (a) in uncoated condition, and (b) with HVOF-spray Cr_3C_2-NiCr coating

scale. However, the concentration of the same is moderate at all the points. The oxide scale for the coated 347H steel seems to be dense and adherent and has retained its continuous contact with the substrate steel even after the oxidation for the 50 cycles. The oxide scale contains mainly chromium along with significant amounts of nickel,

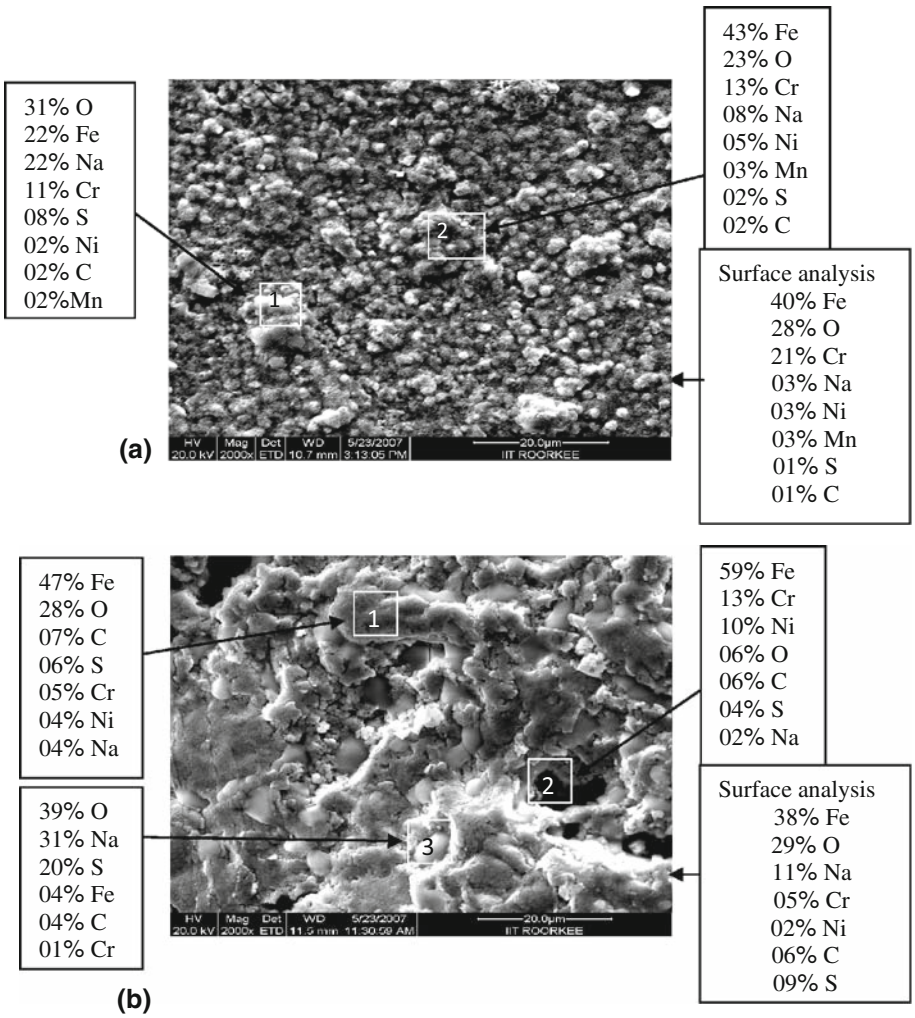

Fig. 13 Surface scale morphology and EDS analysis for the 347H boiler steel subjected to the cyclic oxidation in Na_2SO_4-82%$Fe_2(SO_4)_3$ salt at 700 °C for 50 cycles (a) in uncoated condition, and (b) with HVOF-spray Cr_3C_2-NiCr coating

carbon, and oxygen. This indicates the possibility of formation of oxides and carbides of mainly chromium in the oxide scale (Fig. 14b).

3.8 Molten Salt Oxidation

A cross-sectional micrograph showing oxide scale morphology for the bare 347H steel corroded in the molten salt for 50 cycles at 700 °C is shown in Fig. 15(a). It shows a loose oxide scale with a variable thickness. The EDS analysis presents a comparative estimate of elemental compositions at some points in the substrate as well as in the scale. The point analysis across the scale indicates the presence of iron, carbon, and oxygen with comparatively small amounts of chromium, nickel, and sodium. On the other hand, a dense and adherent scale could be seen for the Cr_3C_2-NiCr coated boiler steel subjected to Na_2SO_4-82%$Fe_2(SO_4)_3$ salt induced corrosion for 50 cycles at 700 °C as has been shown in Fig. 15(b). The EDS analysis of the cross section of the coated steel at point 1 reveals that the substrate consists mainly of iron along with some amounts of chromium, nickel, and carbon. From the point 2 onward up to the point 4, a decrease in the amount of iron is noticed, and the scale consists mainly increasing amount of chromium. The outer layer of the scale is found to be consisting mainly of carbon and oxygen with small quantities of chromium and sodium. The substrate steel is found to be unaffected from oxidation.

3.9 X-Ray Mapping of the Scales

3.9.1 Air Oxidation. Composition image (SE) and x-ray mappings of the cross section of the uncoated 347H boiler steel subjected to cyclic oxidation in air at 700 °C for 50 cycles have been shown in Fig 16. The oxide scale has a dense appearance, in general which has a nearly uniform thickness. The scale appears to have loose adherence with the matrix. From the x-ray maps, it is clear that the scale mainly consists of Fe and Cr. Both these elements are found to be coexisting in the scale. Ni and Mn are also seen throughout the scale. Oxygen is found to

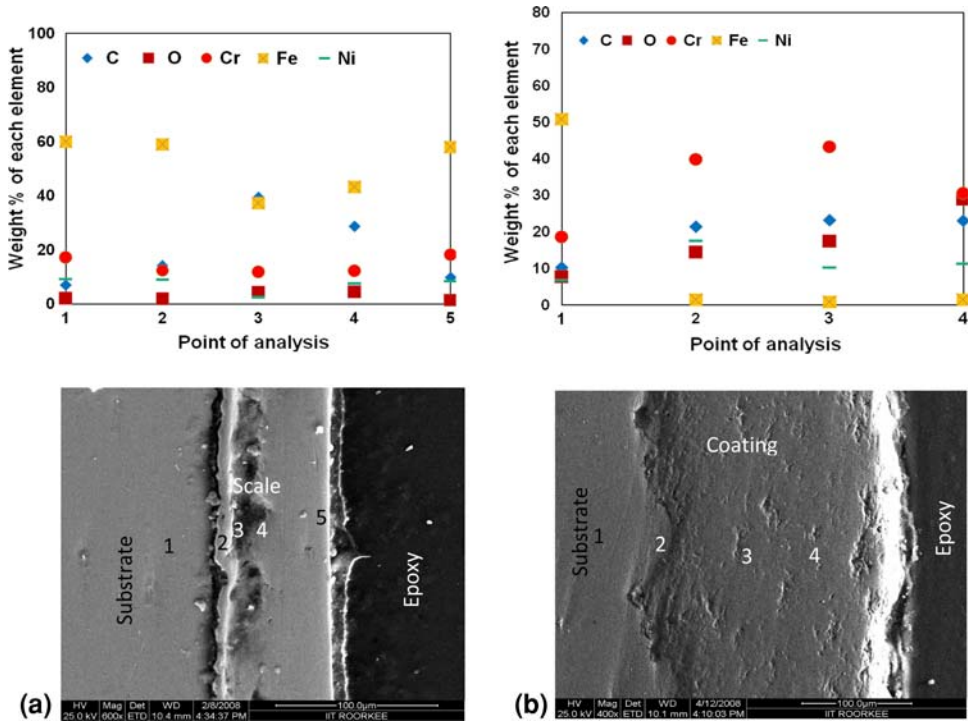

Fig. 14 Oxide scale morphology and variation of elemental composition across the cross section at 347H boiler steel subjected to cyclic oxidation in air for 50 cycles (a) in uncoated condition, and (b) with HVOF-spray Cr_3C_2-NiCr coating

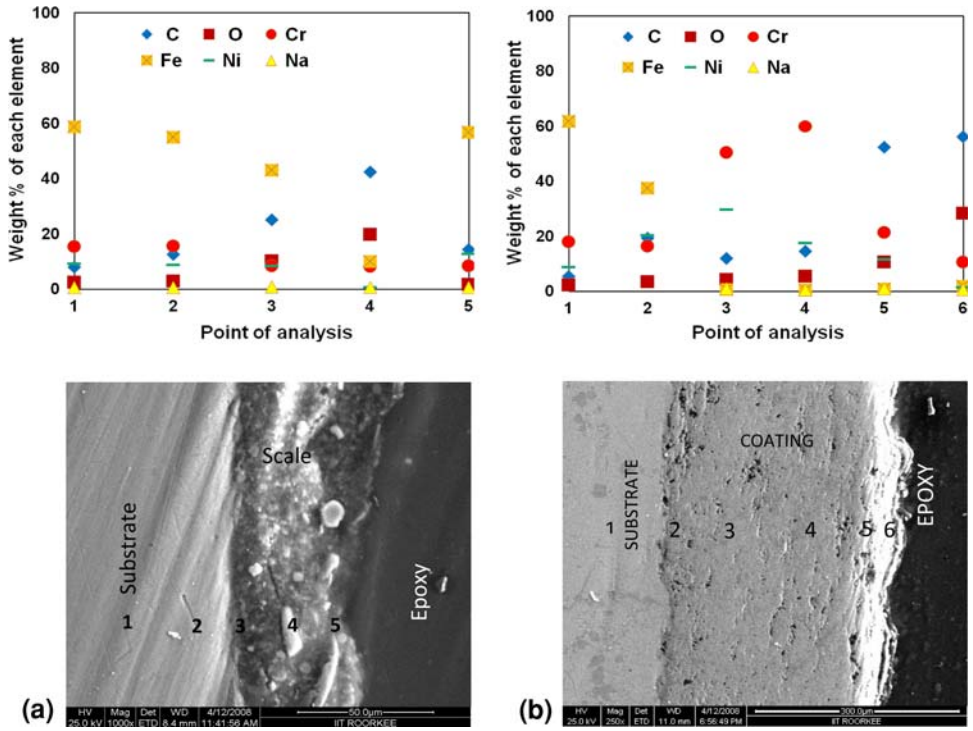

Fig. 15 Oxide scale morphology and variation of elemental composition across the cross section of 347H boiler steel subjected to the cyclic oxidation in Na_2SO_4-82%Fe_2 $(SO_4)_3$ salt at 700 °C for 50 cycles (a) in uncoated condition, and (b) with HVOF-spray Cr_3C_2-NiCr coating

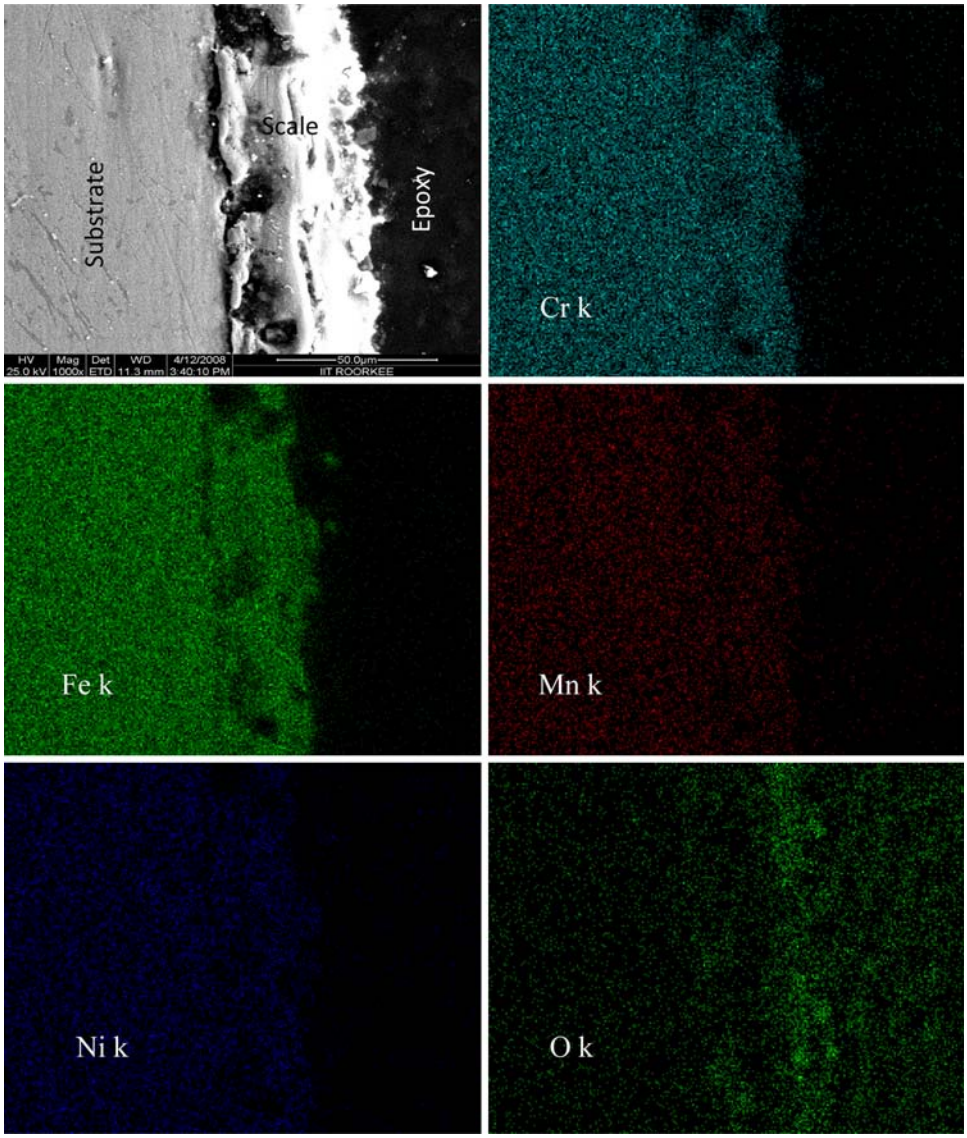

Fig. 16 Composition image (SE) and x-ray mapping of the cross section of the uncoated 347H boiler steel subjected to cyclic oxidation in air at 700 °C for 50 cycles

be higher in concentration in the outer layers of the oxide scale. A similar analysis for the HVOF spray Cr_3C_2-NiCr coated steel case (Fig 17) shows a dense and adherent oxide scale. The x-ray maps indicate that the scale is mainly consisting of Cr and O. Ni is also seen throughout the scale, but in a rarified manner.

3.10 Molten Salt Oxidation

SE and x-ray mappings of the cross section of the uncoated 347H boiler steel subjected to Na_2SO_4-$Fe_2(SO_4)_3$ salt environment at 700 °C for 50 cycles have been shown in Fig 18. X-ray maps clearly indicate that the scale comprises mainly of Fe, Cr, and O. There is also rarified presence of Ni and Si throughout the scale. Na and S are also seen penetrated in the scale, which indicates the onset of the hot corrosion. A corresponding analysis for the Cr_3C_2-NiCr coated case indicates that the oxide scale is mainly containing Cr, Ni, and O. Fe is mainly limited to the substrate and has not shown any diffusion into the scale.

4. Discussion

At high temperatures where WC coatings are not suitable, Cr_3C_2-NiCr coatings have been considered to minimize wear and corrosion (Ref 11). These have high resistance against abrasive wear and low-frictional coefficient from room temperatures up to 850 °C, due to their high thermal stability and oxidation resistance. The corrosion resistance is provided by NiCr matrix while the wear resistance is mainly due to the carbide ceramic phase (Ref 12).

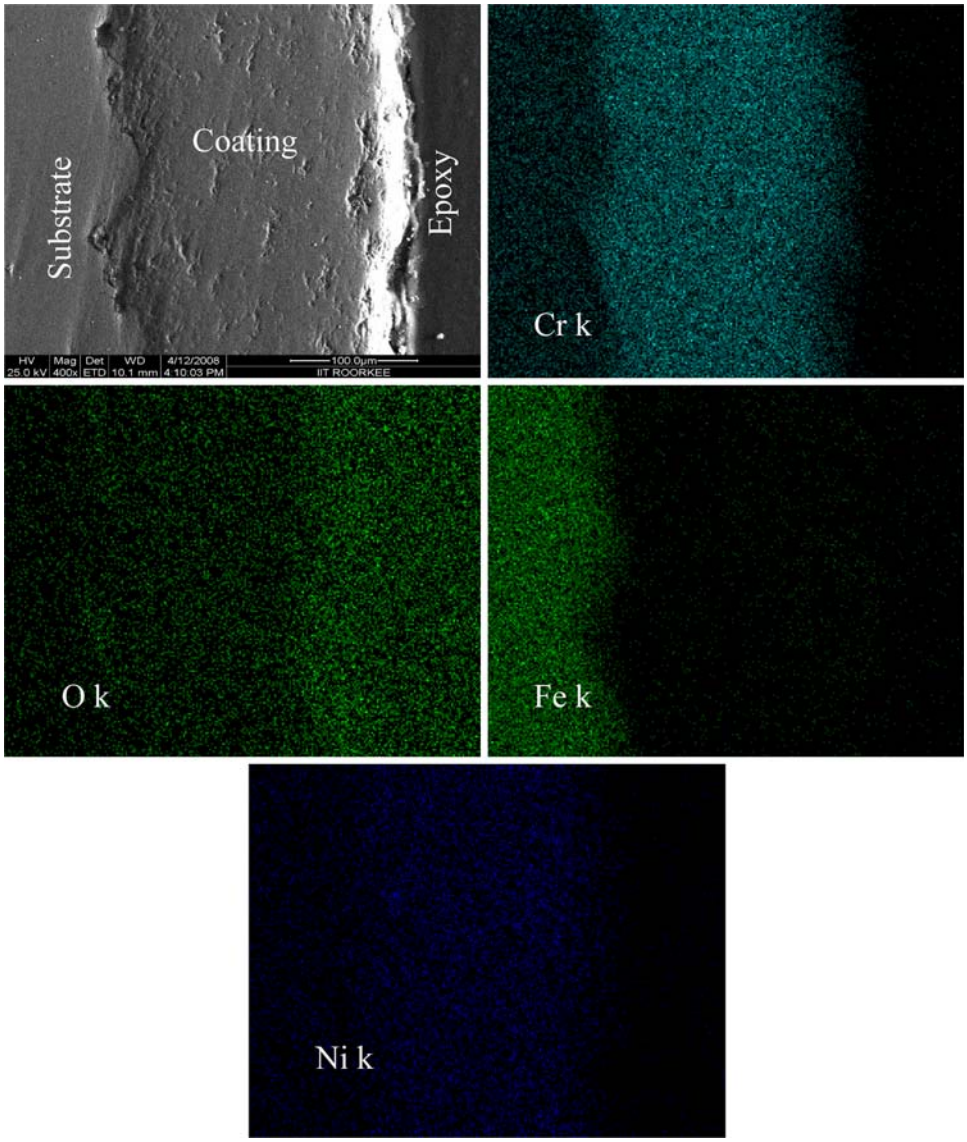

Fig. 17 Composition image (SE) and x-ray mapping of the cross section of the HVOF spray Cr_3C_2-NiCr coated 347H boiler steel subjected to cyclic oxidation in air at 700 °C for 50 cycles

In this study, Cr_3C_2-NiCr coatings were successfully deposited on the given 347H boiler steel. The as-sprayed coating possessed a typical splat like morphology, which is similar to that reported by Matthews et al. (Ref 13) during their long-term carbide development studies on HVOF spray Cr_3C_2-NiCr coatings on mild steel substrates at 900 °C. The XRD analysis of the coating surface showed the presence of Cr_3C_2, Cr_7C_3 (formed perhaps by decarburisation of Cr_3C_2), and Cr_3Ni_2 phases in its composition. Some medium peaks related to CrNi phase were also seen. Similar phases have also been reported by Sahraoui et al. (Ref 14), Sidhu et al. (Ref 15), and Guilemany et al. (Ref 16). Murthy et al. (Ref 17) also reported the formation of Cr_7C_3 and NiCr phases for the HVOF spray $80Cr_3C_2$-20NiCr coatings on mild steel substrates which was also reported earlier (Ref 18-20) for the composition Cr_3C_2-25(NiCr).

Weight-change data for the HVOF-spray Cr_3C_2-NiCr coated and bare boiler steel (Fig. 6 and 7) show the loss in weight values for all the investigated cases during the exposure time of 50 cycles. This weight loss may be attributed to the high-temperature interactions of metal oxide and Na_2SO_4 in O_2 (g) indicating the expulsion of S-oxide gases and or vaporization of some volatile compounds (Ref 21). Lai (Ref 22) has also reported oxidation weight losses for this steel. The coated 347H boiler steel showed better air oxidation as well as molten salt corrosion resistance in comparison to its uncoated counterpart. The bare 347H steel showed accelerated hot corrosion in Na_2SO_4-82%Fe_2 $(SO_4)_3$ salt environment at 700 °C. However, after the deposition of the coating, the corrosion weight loss decreased by 53% which is significant. Whereas, it is interesting to note that the reduction in

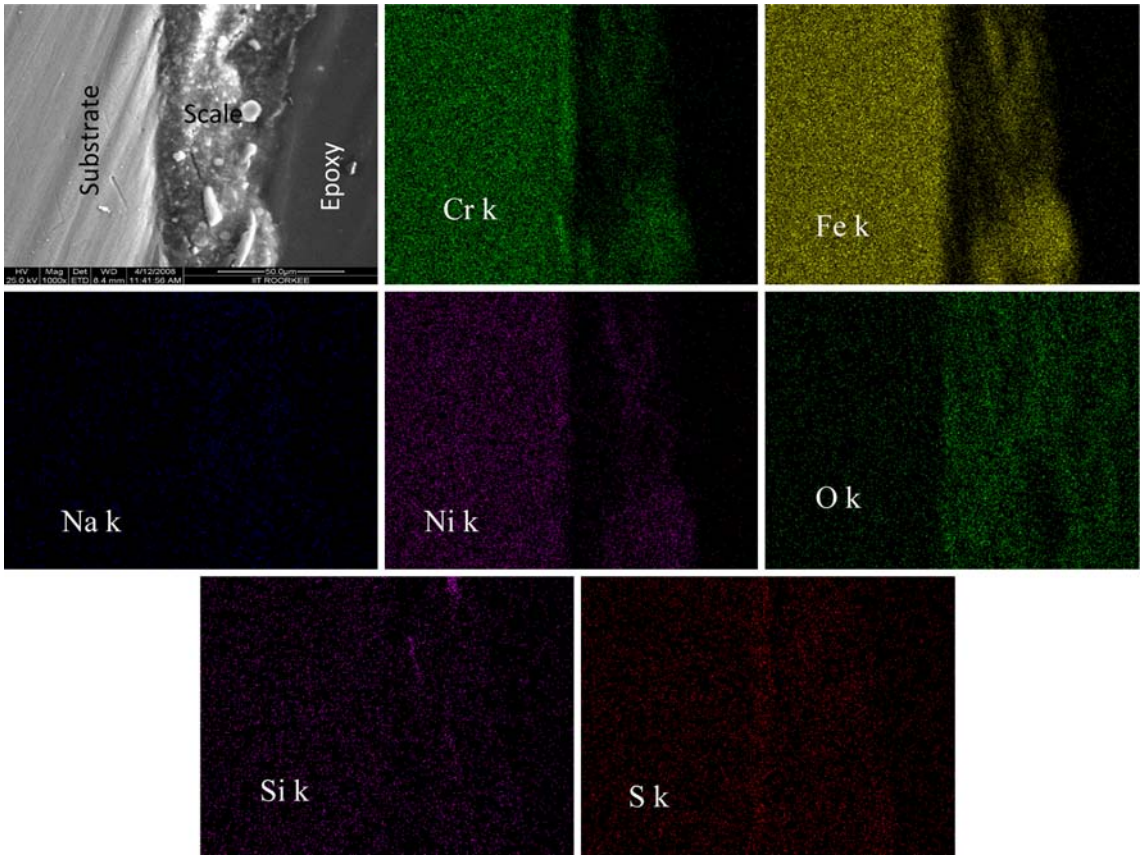

Fig. 18 Composition image (SE) and x-ray mapping of the cross section of the uncoated 347H boiler steel subjected to Na_2SO_4-$Fe_2(SO_4)_3$ salt environment at 700 °C for 50 cycles

oxidation loss is only 15% after the deposition of the coating which is significantly lower than that observed during the molten salt corrosion. It has also been observed that the molten salt corrosion loss for the 347H steel is significantly higher than its loss due to the air oxidation. On the other hand after the deposition of the coating, the molten salt corrosion loss is comparatively lesser than the air oxidation loss. Therefore, from the ongoing discussion, it may be concluded that the HVOF-spray Cr_3C_2-NiCr coating showed protective behavior in both the environments of the study at 700 °C under cyclic conditions. Furthermore, the observed spallation of the oxide scales for the coated samples in both the environments of study could be attributed to the mismatch between the coefficients of thermal expansion of the substrate, coating and oxides formed. However, the extent of this spallation was marginal. The various phases identified from the XRD patterns of the oxidized bare 347H steel in air at 700 °C for 50 cycles are shown in Fig. 8. FeNi and Ni, Fe were observed as the main peaks, whereas Fe_2O_3 and Cr_2O_3 were appeared as weak phases. This is further supported by surface and cross-sectional EDS analyses. Further from the x-ray maps also, it is clear that the scale mainly consists of Fe and Cr. Oxygen is found to be higher in concentration in the outer scale. On the other hand, the XRD analysis revealed the presence of Cr_2O_3 and Cr_7C_3 as very strong phases along with Cr_3C_2 as a strong phase and Cr_2C, Cr_3O_4, and Cr_3Ni_2i as medium and low intensity phases in the surface scale of the air oxidized Cr_3C_2-NiCr-coated boiler steel. Similar phases have also been reported by Matthews et al. (Ref 13). The surface EDS analysis of the coating further showed the presence of Cr as the main element along with significant amounts of Ni and O and thus supports the formation of these phases. This is further supported by both the cross-sectional EDS as well as x-ray mapping analyses. Moreover, the surface scale formed on Cr_3C_2-NiCr coated boiler steel is dense and adherent by and large, and has retained its continuous contact with the substrate steel during the course of study.

The XRD diffractograms for the uncoated and coated boiler steel after exposure to the given salt environment at 700 °C for 50 cycles are depicted in Fig. 10 and 11, respectively, on reduced scales. Fe_2O_3 and Cr_2O_3 were the strong phases which are found to be present in the hot-corroded 347H boiler steel. Also, NiO and Na_2O were observed as weak phases. This has also been indicated by the surface EDS analysis. The cross-sectional EDS analysis also indicates the presence of iron, carbon, and oxygen with comparatively small amounts of chromium, nickel, and sodium in the oxide scale. The x-ray maps further endorse that the scale comprises mainly of Fe, Cr, and O. Na and S were also seen penetrated in the scale, which

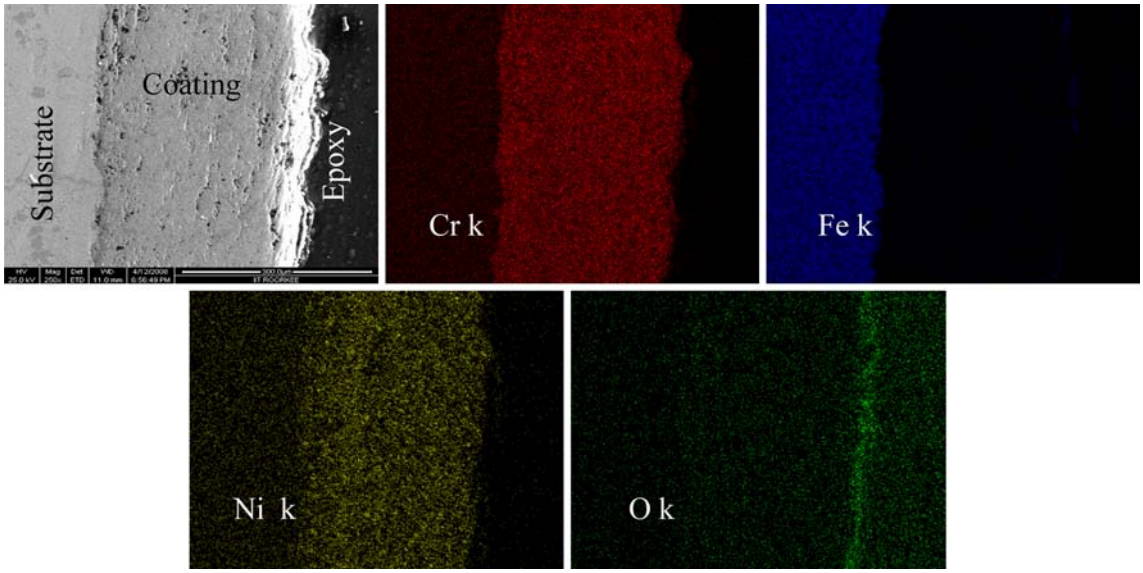

Fig. 19 Composition image (SE) and x-ray mapping of the cross section of the HVOF-spray Cr_3C_2-NiCr coated 347H boiler steel subjected to Na_2SO_4-$Fe_2(SO_4)_3$ salt environment at 700 °C for 50 cycles

indicates the onset of the hot corrosion. The identification of Fe_2O_3 in the scales of uncoated steel indicated that nonprotective conditions were established when Na_2SO_4-82%$Fe_2(SO_4)_3$ molten salt was present on the surface. The formation of this nonprotective phase (Fe_2O_3) has also been reported by Sidhu et al. (Ref 15) during their hot corrosion study on a boiler tube steel namely, ASTM-SA210 grade A1 (GrA1) in molten salt (Na_2SO_4-60%V_2O_5) environment. On the other hand, the Cr_3C_2-NiCr coating has shown the formation of Fe_2O_3, Cr_2O_3, Cr_7C_3, and Cr_2C phases in its oxide scale as indicated by the XRD analysis. The cross-sectional EDS analysis of the coated steel has also confirmed the formation of these phases. Further these results were also supported by x-ray mapping analysis. The formation of a thick chromium layer in the scale as revealed by the x-ray maps (Fig. 19) might have contributed for the better hot corrosion resistance.

5. Conclusions

1. Cr_3C_2-NiCr coatings could be obtained on 347H boiler tube steels by the HVOF-spray process, and the coatings were found to be promising from the point of view of oxidation and hot corrosion resistance.
2. The as-sprayed Cr_3C_2-NiCr coating is found to have a morphology consisting of irregular shaped splats. The splats have variable shapes and sizes, which are interconnected.
3. The bare 347H steel suffered accelerated oxidation during exposure at 700 °C in air as well as molten salt environment in comparison with its coated counterparts. It has also been observed that the molten salt corrosion loss for the 347H steel was significantly higher than its loss due to the air oxidation.
4. The HVOF-spray Cr_3C_2-NiCr coating was found to be successful in maintaining its adherence in both the environments. The surface scales were also found to be intact. The coated 347H boiler steel showed better air oxidation as well as molten salt corrosion resistance in comparison with its uncoated counterpart. The formation of chromium rich oxide scale might have contributed for the better hot corrosion/oxidation resistance in the coated steel.
5. The HVOF-spray Cr_3C_2-NiCr coating performed better in the molten salt [Na_2SO_4-82%$Fe_2(SO_4)_3$] environment in comparison with that in the air environment.

Acknowledgments

Harpreet Singh et al thankfully acknowledge the research grant from Department of Science and Technology, New Delhi (India) under SERC FAST Scheme (File No. SR/FTP/ETA-06/06, Dated March 16, 2006) to carry out this R & D work, titled ''Development of Erosion-Corrosion Resistant Thermal Spray Coatings for Power Plant Boilers.''

References

1. J. Mostaghimi, S. Chandra, R. Ghafouri-Azar, and A. Dolatabadi, Modelling Thermal Spray Coating Processes: A Powerful Tool in Design and Optimization, *Surf. Coat. Technol.*, 2003, **163-164**, p 1-11
2. J. Stokes and L. Looney, HVOF System Definition to Maximize the Thickness of Formed Components, *Surf. Coat. Technol.*, 2001, **148**, p 18-24
3. J.M. Perry, A. Neville, and T. Hodgkiess, A Comparison of the Corrosion Behaviour of WC-CoCr and WC-Co HVOF Thermally

Sprayed Coatings by In Situ Atomic Force Microscopy (AFM), *J. Therm. Spray Tech.*, 2002, **11**(4), p 536-541
4. J.M. Guilemany, J.M. Miguel, S. Vizcaino, C. Lorenzana, J. Delgado, and J. Sanchez, Role of Heat Treatments in the Improvement of the Sliding Wear Properties of Cr_3C_2-NiCr Coatings, *Surf. Coat. Technol.*, 2002, **157**, p 207-213
5. M.H. Staia, T. Valente, C. Bartuli, D.B. Lewis, C.P. Constable, A. Roman, J. Lesage, D. Chicot, and G. Mesmacque, Part II: Tribological Performance of Cr_3C_2-25%NiCr Reactive Plasma Sprayed Coatings Deposited At Different Pressures, *Surf. Coat. Technol.*, 2001, **146-147**, p 563-570
6. D.Y. Kim and M.S. Han, *Thermal Spray: Practical Solutions for Engineering Problems*, C.C. Berndt, Ed., ASM International, OH, 1996, p 123-128
7. B.Q. Wang, *Surface Modifications Technologies XI*, T.S. Sudarshan et al., Ed., The Institute of Materials, Paris, 1997, p 458-467
8. L.M. Berger, P. Vuoristo, T. Mantyla, and W. Gruner, *Thermal Spray; Meeting the Challenges of the 21st Century*, C. Coddet, Ed., ASM International, Material Park, Nice, 1998, p 75-82
9. B.G. Seong, S.Y. Hwang, and K.Y. Kim, High Temperature Corrosion of Recuperators used in Steel Mills, *Surf. Coat. Technol.*, 2000, **126**, p 256-265
10. N. Hussain, K.A. Shahid, I.H. Khan, and S. Rahman, Oxidation of High-Temperature Alloys (Superalloys) at Elevated Temperatures in Air: I, *Oxid. Met.*, 1994, **41**(3-4), p 251-269
11. S. Matthews, M. Hyland, and B. James, Microhardness Variation in Relation to Carbide Development in Heat Treated Cr_3C_2-NiCr Thermal Spray Coatings, *Acta Mater.*, 2003, **51**, p 4267-4277
12. L. Pawlowski, *The Science and Engineering of Thermal Spray Coatings*, Wiley & Sons, 1995, 414 pp. ISBN 0-47-159253-2
13. S. Matthews, M. Hyland, and B. James, Long-Term Carbide Development in High-Velocity Oxygen Fuel/High-Velocity Air Fuel Cr_3C_2-NiCr Coatings Heat Treated at 900 °C, *J. Therm. Spray Tech.*, 2004, **13**(4), p 526-536
14. T. Sahraoui, N.E. Fenineche, G. Montavon, and C. Coddet, Structure and Wear Behaviour of HVOF Sprayed Cr_3C_2-NiCr and WC-Co Coatings, *Mater. Design*, 2003, **24**, p 309-313
15. H.S. Sidhu, B.S. Sidhu, and S. Prakash, Mechanical and Microstructural Properties of HVOF Sprayed WC-Co and Cr_3C_2-NiCr Coatings on the Boiler Tube Steels Using LPG as the Fuel Gas, *J. Mater. Process. Technol.*, 2006, **171**, p 77-82
16. J.M. Guilemany, N. Espallargas, P.H. Suegama, and A.V. Benedetti, Comparative Study of Cr_3C_2-NiCr Coatings Obtained by HVOF and Hard Chromium Coatings, *Corros. Sci.*, 2006, **48**, p 2998-3013
17. J.K.N. Murthy and B. Venkataraman, Abrasive Wear Behaviour of WC-CoCr and Cr_3C_2-20(NiCr) Deposited by HVOF and Detonation Spray Processes, *Surf. Coat. Technol.*, 2006, **200**, p 2642-2652
18. P. Vuoristo, K. Niemi, A. Makela, and T. Mantyla, *Proceedings of the 7th National Thermal Spray Conference*, Boston, MA, 20-24 June 1994, p 121-126
19. I.M. Guilemany and J.A. Calero, *Surface Modification Technologies*, Vol XI, T.S. Sudarshan, M. Jeandin, and K.A. Khor, Ed., The Institute of Materials, London, 1998, p 81
20. J. Takeuchi, Y. Murata, Y. Harada, T. Nomita, S. Nakhama, and T. Go, *Proceedings of the 15th International Thermal Spray Conference*, 25-29 May 1998, France, 1425 p
21. M. Mobin, A.U. Malik, S. Ahmed, S.K. Hasan, and M. Ajmal, Studies on the Interactions of Metal Oxides and Na_2SO_4 at 1100 and 1200 K in Oxygen, *Bull. Mater. Sci.*, 1996, **19**(5), p 807-821
22. G.Y. Lai, *High Temperature Corrosion of Engineering Alloys*, ASM International, USA, 1990